

**Pathology of idiopathic pulmonary fibrosis assessed by a combination of micro-computed tomography, histology, and immunohistochemistry**

Naoya Tanabe<sup>1,2\*</sup>, John E. McDonough<sup>3,4\*</sup>, Dragoş M. Vasilescu<sup>1\*</sup>, Kohei Ikezoe<sup>1,2</sup>, Stijn E. Verleden<sup>4</sup>, Feng Xu<sup>1</sup>, Wim A Wuyts<sup>4</sup>, Bart M. Vanaudenaerde<sup>4</sup>, Thomas V. Colby<sup>5</sup>, James C. Hogg<sup>1</sup>

<sup>1</sup> Centre for Heart and Lung Innovation, at St. Paul's Hospital, University of British Columbia, Vancouver, BC, Canada

<sup>2</sup> Department of Respiratory Medicine, Graduate School of Medicine, Kyoto University, Kyoto, Japan

<sup>3</sup> Department of Internal Medicine, Section of Pulmonary, Critical Care & Sleep Medicine, Yale School of Medicine, New Haven, CT, USA

<sup>4</sup> KU Leuven, Department of Chronic disease, metabolism and aging, Laboratory of Respiratory diseases, Leuven, Belgium

<sup>5</sup> Department of Laboratory Medicine and Pathology (Emeritus), Mayo Clinic, Scottsdale, AZ, USA

\* Authors contributed equally to this work.

**Number of text pages:** 23

**Number of tables:** 4

**Number of figures:** 3

**Short running head (40 characters or less):** Pathologist's scores and microCT in IPF

**Grant numbers and sources of support:** NT received the Dr. K. K. Pump Fellowship of the BC Lung Association. DMV received a fellowship award from the Parker B. Francis

foundation. SEV is supported by a post doctoral fellowship of FWO (12G8718N) and a grant from KU Leuven (C24/18/073)

**Disclosures:** Authors have no conflict of interest to declare.

**Corresponding author:**

Naoya Tanabe, MD, PhD

Centre for Heart and Lung Innovation, St. Paul's Hospital, University of British Columbia, Vancouver, BC, Canada

166-1081 Burrard St, Vancouver, B.C., Canada, V6Z 1Y6

(Current address)

Department of Respiratory Medicine, Graduate School of Medicine, Kyoto University, Kyoto, Japan

54 Kawahara-cho, Shogoin, Sakyo-ku, Kyoto 606-8507, Japan

Email: ntana@kuhp.kyoto-u.ac.jp

**Abstract (Unstructured, 218 /220 words)**

Idiopathic pulmonary fibrosis (IPF) is a fibrotic disease showing the histology of usual interstitial pneumonia (UIP). While the pathologist's visual inspection is central in histological assessments, three-dimensional microCT assessment may complement pathologist's scoring. This study examined associations between the histopathological features of UIP/IPF in explanted lungs and quantitative microCT measurements including alveolar surface density, total lung volume taken up by tissue (tissue%), and terminal bronchiolar number. Sixty frozen samples from 10 air-inflated explanted lungs with severe IPF and 36 samples from 6 donor control lungs were scanned with microCT and processed for histology. An experienced pathologist scored 3 major UIP criteria (patchy fibrosis, honeycomb, and fibroblastic foci), 5 additional pathological changes such as emphysema, and immunohistochemical staining for CD68, CD4, CD8, and CD79a positive cells, graded on a 0-3+ scale. The alveolar surface density and terminal bronchiolar number decreased and the tissue% increased in IPF compared to controls. In lungs with IPF, lower alveolar surface density and higher tissue% were correlated with greater scores of patchy fibrosis, fibroblastic foci, honeycomb, CD79a-positive cells, and lymphoid follicles. A decreased number of terminal bronchioles was correlated with honeycomb score, but not with the other scores. The three-dimensional microCT measurements reflect the pathological UIP/IPF criteria and further suggest that the reduction in the terminal bronchioles may be associated with honeycomb cyst formation.

**Keywords:** MicroCT, Interstitial lung disease, lung, airway, pulmonary fibrosis

69

70 **List of abbreviation:**

71 IPF = Idiopathic pulmonary fibrosis

72 Lm = Mean linear intercept

73 Tissue% = total lung volume taken up by tissue

74 UIP = Usual interstitial pneumonia

75

76

77 This paper includes an online supplemental video.

78

## Introduction

Idiopathic pulmonary fibrosis (IPF) is a chronic fibrotic disease characterized by a rapid decline in lung function and poor prognosis<sup>1</sup>. The ATS/JRS/and Latin american (ALAT) guidelines all recommended for the diagnosis and management<sup>2</sup> based on an integrative multidisciplinary assessment of clinical information, radiological assessment, histopathologic diagnosis, but while diagnosis can be confirmed without histology in cases that present features of IPF including honeycomb cysts on high resolution computed tomography (HRCT)<sup>2</sup>, histological assessment remains important especially for diagnosing the early stage of IPF and also for improving understanding of the pathogenesis of the disease.

The histopathological changes in IPF are characterized by patchy dense fibrosis that is often accompanied by honeycomb cyst formation<sup>2</sup>. Proliferating fibroblasts and myofibroblasts produce collagen in the active regions of fibroplasia, termed fibroblastic foci<sup>3-5</sup>. In contrast, the infiltration of inflammatory immune cells into fibrotic regions is generally considered to be mild<sup>2</sup>. However, recent histology and gene expression analyses have suggested that a B cell-mediated immune response and lymphoid follicles formations may be associated with fibrosis<sup>6-9</sup>.

The pathologist's visual scoring of UIP/IPF features on lung samples from surgical lung biopsy is essential in histological assessment<sup>1,2</sup>. Although the morphometric approach has been less used in the examination of IPF lungs compared to other lung diseases such as COPD<sup>10-13</sup>, studies have suggested that alveolar collapse onto the alveolar duct mainly contributes to a reduction in alveolar surface area and impairs diffusion capacity in patients with IPF<sup>14-16</sup>. Nonetheless, little remains known regarding direct associations between histologic features of UIP/IPF and quantitative morphometric indices, including the mean linear intercept (Lm), total lung volume taken up by tissue (tissue%), alveolar surface density defined as alveolar surface area per lung volume<sup>17</sup>.

The introduction of micro-computed tomography (microCT) has enabled three-dimensional (3D) morphological assessments of lung tissues that are very difficult to achieve with conventional histology<sup>12, 13, 18, 19</sup>. In addition, microCT scans of frozen air-inflated tissue enable quantitative assessment without shrinkage and physical cutting of tissues<sup>20</sup>. Mai et al.<sup>16</sup> combined CT, microCT, and histological assessments, and showed that fibrosis and honeycomb cysts formation in IPF extends from the peripheral to the central region of the pulmonary lobules. Further, McDonough et al.<sup>21</sup> presented preliminary microCT based analysis of the complex relationship between honeycomb cysts and conducting airways at the American Thoracic Society International Conference which suggested that the honeycomb cyst formation could be a result of airway remodeling. Very recently, Verleden et al.<sup>22</sup> proposed the importance of the small airway disease in IPF by showing that the numbers of the terminal bronchioles (defined as the last generation of the conducting airways) were reduced in lungs with end stage IPF compared to control lungs. Collectively, these findings have demonstrated that quantitative morphometric microCT measurements complement the pathologist's visual inspections of lungs with IPF.

The aim of this study was to extend the understanding of the pathology of UIP/IPF lungs by investigating the relationship between the experienced pathologist's scorings of histological features such as honeycomb cysts and microCT measurements of alveolar surface density, tissue%, Lm, and the number of the terminal bronchioles.

## **Materials and Methods**

**Informed consent:** was obtained either directly from the patient or from the next of kin of the donors that served as controls under conditions approved by the ethical (S52174) and biosafety (MS20101571) committees at the Katholieke Universiteit Leuven and accepted by all the other participating institutions.

**Protocol:** A diagnosis of IPF was based on the current ATS/ERS/JRS/ATLT guidelines that include dominant airway-centered changes as an exclusion criterion<sup>1, 2</sup>. The major features of this protocol have been described in detail elsewhere<sup>9, 22, 23</sup>. Briefly intact lung specimens donated by patients with very severe IPF treated by lung transplantation and unused donor lungs that served as controls were inflated with air and frozen solid with liquid nitrogen vapor. The specimen was kept frozen while cutting it into 2 cm thick transverse slices. Two lung tissue samples were obtained from either the upper, middle, and lower part of the lung (n=6 per lung) to compare samples with different severity of the disease<sup>9, 22, 23</sup>.

**MicroCT-based morphometric quantification:** The tissue samples were kept frozen while scanned at 9.98  $\mu\text{m}$  voxel resolution with a SkyScan 1172 scanner (Kontich, Belgium)<sup>22</sup>. As previously described, image thresholding was applied to separate tissue and airspaces. The tissue segmentation was used to compute tissue% and alveolar surface density (defined as alveolar surface area per volume of lung<sup>9, 23</sup>). The airspace segmentation was used to compute the mean airspace size (mean linear intercept, Lm) by measuring and averaging interalveolar wall distances<sup>22</sup>. The terminal bronchioles were defined as the last generation of conducting bronchioles and counted manually in the microCT scans of each sample. The number of terminal bronchioles per ml of lung was calculated by dividing the number per sample by the sample volume<sup>13, 20</sup>.

**Histology:** The pathologist's scoring was performed in the present study using histological sections obtained in the previous IPF study<sup>22</sup>. Following microCT imaging, portions of the frozen samples were fixed in alcohol-based formalin at -20°C overnight, warmed to room temperature, and then processed into paraffin blocks from which histological sections were cut and stained with H&E and Movat Pentachrome stains. As shown in Figure 1, these histological sections were examined by an experienced pulmonary pathologist (TVC) who scored 8 pathological features that consisted of the 3 major UIP criteria including patchy fibrosis,

honeycomb cyst formation, and fibroblastic foci, as well as 5 additional pathological changes including emphysema, degree of inflammation, hyaline membrane formation, lymphoid follicles, and respiratory bronchiolitis, all on a 0-3+ scale. In addition, other portions of the frozen samples were briefly warmed to -1°C, vacuum embedded in the optimum cutting temperature compound (OCT, SAKURA FINETEK), immediately returned to -80°C, and cut into serial frozen sections (8 µm thick) for immunohistochemistry. These sections were stained with primary antibodies for CD68 (DAKO, M0876, 1:200 dilution), CD4 (DAKO, M7310, 1:200 dilution), CD8 (DAKO, M7103, 1:400 dilution), and CD79a (DAKO, M7050, 1:200 dilution) as previously reported<sup>22</sup>. These sections were also scored by the same pathologist on a 0-3+ scale.

**Statistical Analysis:** Data are expressed as mean ± standard deviation. Statistical analysis was performed with the R statistical program (R Core Team: R: A Language and Environment for Statistical Computing. URL <http://www.R-project.org/>. accessed 2019 Nov 1. version 3.4.1). The Spearman correlation tests and Mann Whitney comparison were used for correlation tests and group comparisons, respectively. Multiple comparisons were performed with Wilcoxon tests with Holm correction.

## Results

Table 1 shows that there is no difference in age, sex, height, or weight between the patients with IPF and the control subjects. Table 2 summarizes microCT and histological scores. Alveolar surface density and the number of terminal bronchioles /ml lung were lower, while tissue% and Lm were higher in IPF compared to controls. In addition, CD68, CD4, CD8, and CD79a positive cells were greater in IPF than controls. Supplemental figure 1 demonstrates that the significant difference between IPF and controls was also present when comparing microCT indices in the upper, middle, and lower regions separately.



Figure 2A and B show examples of histological regions with and without honeycomb formation (score 0 and 1, respectively) that were registered to the microCT scans. Figure 2C and D show that the alveolar surface density and number of terminal bronchioles were lower in the honeycomb regions (Score $\geq$ 1) than in the non-honeycomb regions (Score=0). This finding was visualized on Figure 2E and a video that shows a microCT stack of the same sample as used in Figure 2B and E (Supplemental video 1). The video shows that many branches of the small airway tree (pink) were located in the “normal” appearing regions, but not in the honeycomb region, and that the conducting airway leading into the honeycomb region was directly connected to those severely distorted airspaces (orange). Further, Figure 3 shows that the decreases in the alveolar surface density and number of terminal bronchioles in the honeycomb region were also confirmed in a subanalysis that included non-emphysematous IPF samples (histological emphysema score =0) and controls.

Table 3 shows Spearman correlation coefficients between microCT indices and pathological scores in IPF samples (n=59). Decreased alveolar surface density and increased tissue% and Lm on microCT were correlated with the histological scores of patchy fibrosis, fibroblastic foci, and honeycomb. In contrast, decreased number of the terminal bronchioles was correlated with an increased score of honeycomb, but not with patchy fibrosis and fibroblastic foci.

Table 4 shows Spearman correlation coefficients between microCT indices and scores of lymphoid cells in IPF samples (n=60). Increased tissue% was correlated with increased scores for CD68, CD4, CD8, and CD79a positive cells and lymphoid follicles, whereas Lm and the number of terminal bronchioles were not associated with any of the scores of immune cells and lymphoid follicles.

## Discussion

204           This study compared standard histopathological criteria of UIP/IPF and quantitative  
205 morphological measures obtained from microCT. The microCT findings of decreased alveolar  
206 surface density and increased tissue% were positively associated with the pathologist's  
207 scoring of patchy fibrosis, fibroblastic foci, honeycomb formation, infiltration of CD79a-  
208 positive lymphocytes, and lymphoid follicle formation. Furthermore, a combination of  
209 histological assessment and the three-dimensional microCT information revealed that a  
210 reduction in the number of terminal bronchioles was associated with honeycomb formation,  
211 but not with patchy fibrosis or fibroblastic foci. These findings indicate that three-dimensional  
212 morphometric assessment via microCT can be used to complement the pathologist's visual  
213 inspection to by showing the pathological relationship between the peripheral airways and  
214 parenchyma in lungs with IPF.

215           From a histopathological perspective, UIP/IPF lungs are characterized by spatially  
216 heterogeneous fibrosis with fibroblastic foci and honeycomb lesion<sup>1-3</sup>, and from a  
217 physiological perspective, IPF lungs are characterized by impaired diffusion capacity which  
218 affects the mortality<sup>24</sup>. This structure-function relationship has been explained by multiple  
219 morphometric studies showing that a collapse of alveoli onto the alveolar ducts in IPF lung  
220 leads to a reduction of alveolar surface area<sup>14, 15, 25</sup>. However, to the best of knowledge, no  
221 prior report has tested the direct relationship between the pathological UIP/IPF criteria and  
222 morphometric assessment of IPF lung. Therefore, the close correlations between alveolar  
223 surface density, tissue%, and the histopathological scores of UIP/IPF presented here provide  
224 an explanation for the clinically relevant impairment in diffusion capacity present in IPF  
225 patients.

226           The widely accepted hypothesis that IPF is generally a parenchymal disease in which  
227 the airways are spared was recently challenged by a microCT-based study that showed a loss  
228 of the terminal bronchiole number already occurs in minimal fibrotic regions in lungs with

IPF compared to controls<sup>22</sup>. Since the terminal bronchioles are located in the centre of the secondary lobules, these recent microCT findings have raised the question if there is an interaction between small airway disease, such as loss of the terminal bronchioles, and parenchymal pathology, such as alveolar collapse. The present study sheds light on this issue by showing that the loss of terminal bronchioles is associated with honeycomb formation, but not with patchy fibrosis, which leads to the conclusion that these might be two somewhat separate process. This finding is consistent with the hypothesis proposed by Evans et al.<sup>26</sup> that the peripheral airway injury is associated with honeycomb cyst formation independent of fibroproliferation in the parenchyma. In addition, although COPD studies have shown a close association between emphysema and a reduction in the terminal bronchioles<sup>13, 27, 28</sup>, the reduced number of terminal bronchioles in the honeycomb regions was confirmed even in the subanalysis that excluded IPF samples with emphysema (histological score  $\geq 1$ ).

Furthermore, the supplemental video 1 provided portrays the 3D spatial relationship between the small conducting airways and microscopic honeycomb regions, which on the conventional 2D histological sections would be difficult to detect. The 3D visualization demonstrates that the conducting airways are directly connected to the air spaces within the honeycomb regions. This finding suggests that the potential airways present within the honeycomb region are remodeled beyond recognition, and the small airways might be an origin of honeycomb cysts in IPF. This concept requires further detailed investigation which is beyond the scope of the present study.

Staats et al.<sup>29</sup> showed that a histologic finding of bronchiolectasis is associated with honeycomb score on high-resolution CT (HRCT), and Walsh et al.<sup>30</sup> showed that traction bronchiectasis on HRCT is closely associated with fibroblastic foci profusion on histology. These suggest that traction bronchiectasis and honeycombing are part of a “continuous spectrum of lung remodeling” as noted in clinical observations<sup>31</sup>, and are in line with the

present microCT findings that demonstrate a direct communication between the small airway tree and honeycomb regions in lungs with IPF.

Together with previous findings that the polymorphism in the promoter region of the MUC5B gene which regulates mucin production from bronchiolar epithelium is associated with the pathogenesis of IPF<sup>26, 32</sup> and the honeycomb regions are lined with bronchiolar-like epithelium<sup>33</sup>, we speculate that the terminal bronchiole remodeling might be involved in the honeycomb formation.

This study used a single histological section for each tissue sample. Although microscopic pathologies could vary throughout the tissue sample, it is speculated that within-sample variation is smaller than the inter-samples variation because the cylindrical tissue samples used in this study are relatively small (20 mm high and 14 mm in diameter). Moreover, the close correlation between the pathologist's score of patchy fibrosis and the tissue % on microCT that was obtained from the entire microCT stack, suggests that the single histological section is sufficiently representative of the pathology of the sample core.

Extensive research has shown that a transition of fibroblasts into synthetic myofibroblast, and subsequent deposition of collagen, plays an important role in the progressive fibrotic process after repeated injuries in IPF<sup>34, 35</sup>, however, the role of inflammatory immune cells is not established. Histological studies have found infiltration of inflammatory immune cells such as B cell aggregates<sup>8, 36, 37</sup> while clinical trials using immunosuppressive therapy have consistently failed to show the effectiveness in patients with IPF<sup>38</sup>. A recent study by Verleden et al. showed that the CD79a positive cell infiltration and lymphoid follicle formation are present even in minimal fibrotic regions of IPF lungs<sup>22</sup>. The present finding extends it by demonstrating an association of lymphoid follicle formation score with increased tissue% and decreased alveolar surface density and further supports the

notion that the persistent adaptive immune response contributes to a fibrotic remodeling process in IPF.

Moreover, an increase in CD68-positive cells was associated with the increased tissue% in IPF lungs. This finding is consistent with the hypothesis that macrophages are mainly involved in the pathogenesis of IPF<sup>39, 40</sup> but could also in part reflect the smoking history in all the patients. Macrophages are subcategorized into functional phenotypes such as M1 and M2, and play various roles in the lung, including host defense to external insults and wound healing after injury<sup>41</sup>. Therefore, in addition to staining with CD68 antibody, different approach such as gene expression profiling and flowcytometry should be integrated in a future study to explore the pathogenic roles of each macrophage phenotype in IPF.

There are limitations in the present study worth noting. First, all cases with IPF were from former smokers. Since smoking is a major cause of emphysema that is closely associated with the loss of the terminal bronchioles<sup>13, 27, 28</sup>, the present finding of reduced number of terminal bronchioles in IPF might have been affected by smoking. However, there was no correlation between the pathologist's score for emphysema and the number of terminal bronchioles, suggesting that the influence of smoking-related emphysematous destruction is minimal in this study. Second, the sample number is small and all cases were very-severe IPF that required lung transplantation. In order to broaden insights into disease phenotypes, it would be beneficial if the design of future studies would include lung specimen from subjects with different stages of IPF as well as different smoking status (i.e. both smokers and non-smokers). Third, the static cross-sectional nature of the study limits causal inferences. Therefore, the present study was not able to test whether patchy fibrosis and honeycomb cysts formation induce infiltration of immune cells in IPF lungs or if specific immune cells induce a fibrotic process in IPF lungs.

In conclusion, this is the first study to show that quantitative morphometric microCT measurements of alveolar surface density, tissue%, and Lm are closely associated with the general histo-pathological scoring of patchy fibrosis, fibroblastic foci and honeycomb lesions in IPF. These data suggest that microCT measurements provide a reliable structural assessment of IPF lungs especially since the established major criteria of UIP/IPF are associated with reduced alveolar surface area which potentially impairs diffusion capacity in IPF patients. Furthermore, the three-dimensional microCT evaluation revealed that honeycomb formation, but not patchy fibrosis, is associated with a greater reduction in the number of terminal bronchioles in IPF. Volumetric microCT based quantification of the lung structure complements histological assessment of cellular composition of IPF lungs, and by combining these methods with subsequent gene expression analysis or single cell sequencing it may be possible to identify a novel therapeutic target for this devastating lung disease.

**Acknowledgments:** The authors would like to thank Fanny Chu and Jingwen Pan with their assistance in histological preparation and staining, both from the Centre for Heart Lung Innovation, University of British Columbia.

319

## 320 **References**

- 321 [1] Raghu G, Collard HR, Egan JJ, Martinez FJ, Behr J, Brown KK, Colby TV, Cordier JF,  
322 Flaherty KR, Lasky JA, Lynch DA, Ryu JH, Swigris JJ, Wells AU, Ancochea J, Bouros D,  
323 Carvalho C, Costabel U, Ebina M, Hansell DM, Johkoh T, Kim DS, King TE, Jr., Kondoh Y,  
324 Myers J, Muller NL, Nicholson AG, Richeldi L, Selman M, Dudden RF, Griss BS, Protzko SL,  
325 Schunemann HJ, Fibrosis AEJACoIP: An official ATS/ERS/JRS/ALAT statement: idiopathic  
326 pulmonary fibrosis: evidence-based guidelines for diagnosis and management. Am J Respir Crit  
327 Care Med 2011, 183:788-824.
- 328 [2] Raghu G, Remy-Jardin M, Myers JL, Richeldi L, Ryerson CJ, Lederer DJ, Behr J, Cottin V,  
329 Danoff SK, Morell F, Flaherty KR, Wells A, Martinez FJ, Azuma A, Bice TJ, Bouros D, Brown  
330 KK, Collard HR, Duggal A, Galvin L, Inoue Y, Jenkins RG, Johkoh T, Kazerooni EA, Kitaichi  
331 M, Knight SL, Mansour G, Nicholson AG, Pipavath SNJ, Buendia-Roldan I, Selman M, Travis  
332 WD, Walsh S, Wilson KC, American Thoracic Society ERSJRS, Latin American Thoracic S:  
333 Diagnosis of Idiopathic Pulmonary Fibrosis. An Official ATS/ERS/JRS/ALAT Clinical  
334 Practice Guideline. Am J Respir Crit Care Med 2018, 198:e44-e68.
- 335 [3] Katzenstein AL, Mukhopadhyay S, Myers JL: Diagnosis of usual interstitial pneumonia and  
336 distinction from other fibrosing interstitial lung diseases. Hum Pathol 2008, 39:1275-94.
- 337 [4] Cool CD, Groshong SD, Rai PR, Henson PM, Stewart JS, Brown KK: Fibroblast foci are  
338 not discrete sites of lung injury or repair: the fibroblast reticulum. Am J Respir Crit Care Med  
339 2006, 174:654-8.
- 340 [5] King TE, Jr., Schwarz MI, Brown K, Tooze JA, Colby TV, Waldron JA, Jr., Flint A,  
341 Thurlbeck W, Cherniack RM: Idiopathic pulmonary fibrosis: relationship between  
342 histopathologic features and mortality. Am J Respir Crit Care Med 2001, 164:1025-32.

343 [6] Bringardner BD, Baran CP, Eubank TD, Marsh CB: The role of inflammation in the  
344 pathogenesis of idiopathic pulmonary fibrosis. *Antioxid Redox Signal* 2008, 10:287-301.

345 [7] DePianto DJ, Chandriani S, Abbas AR, Jia G, N'Diaye EN, Caplazi P, Kauder SE, Biswas  
346 S, Karnik SK, Ha C, Modrusan Z, Matthay MA, Kukreja J, Collard HR, Egen JG, Wolters PJ,  
347 Arron JR: Heterogeneous gene expression signatures correspond to distinct lung pathologies  
348 and biomarkers of disease severity in idiopathic pulmonary fibrosis. *Thorax* 2015, 70:48-56.

349 [8] Xue J, Kass DJ, Bon J, Vuga L, Tan J, Csizmadia E, Otterbein L, Soejima M, Levesque MC,  
350 Gibson KF, Kaminski N, Pilewski JM, Donahoe M, Sciurba FC, Duncan SR: Plasma B  
351 lymphocyte stimulator and B cell differentiation in idiopathic pulmonary fibrosis patients. *J*  
352 *Immunol* 2013, 191:2089-95.

353 [9] McDonough JE, Kaminski N, Thienpont B, Hogg JC, Vanaudenaerde BM, Wuyts WA:  
354 Gene correlation network analysis to identify regulatory factors in idiopathic pulmonary fibrosis.  
355 *Thorax* 2018.

356 [10] Tanabe N, Vasilescu DM, Hague CJ, Ikezoe K, Murphy DT, Kirby M, Stevenson CS,  
357 Verleden SE, Vanaudenaerde BM, Gayan-Ramirez G, Janssens W, Coxson HO, Pare PD, Hogg  
358 JC: Pathological Comparisons of Paraseptal and Centrilobular Emphysema in COPD. *Am J*  
359 *Respir Crit Care Med* 2020.

360 [11] Vasilescu DM, Martinez FJ, Marchetti N, Galban CJ, Hatt C, Meldrum CA, Dass C,  
361 Tanabe N, Reddy RM, Lagstein A, Ross BD, Labaki WW, Murray S, Meng X, Curtis JL,  
362 Hackett TL, Kazerooni EA, Criner GJ, Hogg JC, Han MK: Noninvasive Imaging Biomarker  
363 Identifies Small Airway Damage in Severe Chronic Obstructive Pulmonary Disease. *Am J*  
364 *Respir Crit Care Med* 2019, 200:575-81.

365 [12] Tanabe N, Vasilescu DM, McDonough JE, Kinose D, Suzuki M, Cooper JD, Pare PD,  
366 Hogg JC: Micro-Computed Tomography Comparison of Preterminal Bronchioles in  
367 Centrilobular and Panlobular Emphysema. *Am J Respir Crit Care Med* 2017, 195:630-8.



368 [13] McDonough JE, Yuan R, Suzuki M, Seyednejad N, Elliott WM, Sanchez PG, Wright AC,  
369 Gefter WB, Litzky L, Coxson HO, Pare PD, Sin DD, Pierce RA, Woods JC, McWilliams AM,  
370 Mayo JR, Lam SC, Cooper JD, Hogg JC: Small-airway obstruction and emphysema in chronic  
371 obstructive pulmonary disease. *N Engl J Med* 2011, 365:1567-75.

372 [14] Coxson HO, Hogg JC, Mayo JR, Behzad H, Whittall KP, Schwartz DA, Hartley PG, Galvin  
373 JR, Wilson JS, Hunninghake GW: Quantification of idiopathic pulmonary fibrosis using  
374 computed tomography and histology. *Am J Respir Crit Care Med* 1997, 155:1649-56.

375 [15] Lutz D, Gazdhar A, Lopez-Rodriguez E, Ruppert C, Mahavadi P, Gunther A, Klepetko W,  
376 Bates JH, Smith B, Geiser T, Ochs M, Knudsen L: Alveolar derecruitment and collapse  
377 induration as crucial mechanisms in lung injury and fibrosis. *Am J Respir Cell Mol Biol* 2015,  
378 52:232-43.

379 [16] Mai C, Verleden SE, McDonough JE, Willems S, De Wever W, Coolen J, Dubbeldam A,  
380 Van Raemdonck DE, Verbeken EK, Verleden GM, Hogg JC, Vanaudenaerde BM, Wuyts WA,  
381 Verschakelen JA: Thin-Section CT Features of Idiopathic Pulmonary Fibrosis Correlated with  
382 Micro-CT and Histologic Analysis. *Radiology* 2016:152362.

383 [17] Hsia CC, Hyde DM, Ochs M, Weibel ER, Structure AEJTFoQAoL: An official research  
384 policy statement of the American Thoracic Society/European Respiratory Society: standards  
385 for quantitative assessment of lung structure. *Am J Respir Crit Care Med* 2010, 181:394-418.

386 [18] Verleden SE, Vanstapel A, De Sadeleer L, Weynand B, Boone M, Verbeken E, Piloni D,  
387 Van Raemdonck D, Ackermann M, Jonigk DD, Verschakelen J, Wuyts WA: Quantitative  
388 analysis of airway obstruction in lymphangioleiomyomatosis. *Eur Respir J* 2020, 56.

389 [19] Bourdin A, Gamez AS, Vachier I, Crestani B: LAM is another small airway disease:  
390 lessons from microCT. *Eur Respir J* 2020, 56.

391 [20] Vasilescu DM, Phillion AB, Tanabe N, Kinose D, Paige DF, Kantrowitz JJ, Liu G, Liu H,  
392 Fishbane N, Verleden SE, Vanaudenaerde BM, Lenburg ME, Stevenson CS, Spira A, Cooper

393 JD, Hackett TL, Hogg JC: Non-destructive cryo micro CT imaging enables structural and  
 394 molecular analysis of human lung tissue. *J Appl Physiol* (1985) 2016:jap 00838 2016.

395 [21] McDonough JE, Verleden SE, Verschakelen J, Wuyts W, Vanaudenaerde BM: The  
 396 Structural Origin of Honeycomb Cysts in IPF. *D28 RESPIRATORY DISEASE DIAGNOSIS:*  
 397 *PULMONARY FUNCTION TESTING AND IMAGING:* American Thoracic Society, 2018.  
 398 pp. A6388-A.

399 [22] Verleden SE, Tanabe N, McDonough JE, Vasilescu DM, Xu F, Wuyts WA, Piloni D, De  
 400 Sadeleer L, Willems S, Mai C, Hostens J, Cooper JD, Verbeken EK, Verschakelen J, Galban  
 401 CJ, Van Raemdonck DE, Colby TV, Decramer M, Verleden GM, Kaminski N, Hackett TL,  
 402 Vanaudenaerde BM, Hogg JC: Small airways pathology in idiopathic pulmonary fibrosis: a  
 403 retrospective cohort study. *Lancet Respir Med* 2020, 8:573-84.

404 [23] McDonough JE, Ahangari F, Li Q, Jain S, Verleden SE, Herazo-Maya J, Vukmirovic M,  
 405 DeIuliis G, Tzouvelekis A, Tanabe N, Chu F, Yan X, Verschakelen J, Homer RJ, Manatakis  
 406 DV, Zhang J, Ding J, Maes K, De Sadeleer L, Vos R, Neyrinck A, Benos PV, Bar-Joseph Z,  
 407 Tantin D, Hogg JC, Vanaudenaerde BM, Wuyts WA, Kaminski N: Transcriptional regulatory  
 408 model of fibrosis progression in the human lung. *JCI Insight* 2019, 4.

409 [24] King TE, Jr., Tooze JA, Schwarz MI, Brown KR, Cherniack RM: Predicting survival in  
 410 idiopathic pulmonary fibrosis: scoring system and survival model. *Am J Respir Crit Care Med*  
 411 2001, 164:1171-81.

412 [25] Myers JL, Katzenstein AL: Epithelial necrosis and alveolar collapse in the pathogenesis of  
 413 usual interstitial pneumonia. *Chest* 1988, 94:1309-11.

414 [26] Evans CM, Fingerlin TE, Schwarz MI, Lynch D, Kurche J, Warg L, Yang IV, Schwartz  
 415 DA: Idiopathic Pulmonary Fibrosis: A Genetic Disease That Involves Mucociliary Dysfunction  
 416 of the Peripheral Airways. *Physiol Rev* 2016, 96:1567-91.

417 [27] Koo HK, Vasilescu DM, Booth S, Hsieh A, Katsamenis OL, Fishbane N, Elliott WM,  
418 Kirby M, Lackie P, Sinclair I, Warner JA, Cooper JD, Coxson HO, Pare PD, Hogg JC, Hackett  
419 TL: Small airways disease in mild and moderate chronic obstructive pulmonary disease: a cross-  
420 sectional study. *Lancet Respir Med* 2018, 6:591-602.

421 [28] Tanabe N, Vasilescu DM, Kirby M, Coxson HO, Verleden SE, Vanaudenaerde BM,  
422 Kinose D, Nakano Y, Pare PD, Hogg JC: Analysis of airway pathology in COPD using a  
423 combination of computed tomography, micro-computed tomography and histology. *Eur Respir*  
424 *J* 2018, 51.

425 [29] Staats P, Kligerman S, Todd N, Tavora F, Xu L, Burke A: A comparative study of  
426 honeycombing on high resolution computed tomography with histologic lung remodeling in  
427 explants with usual interstitial pneumonia. *Pathol Res Pract* 2015, 211:55-61.

428 [30] Walsh SL, Wells AU, Sverzellati N, Devaraj A, von der Thusen J, Yousem SA, Colby TV,  
429 Nicholson AG, Hansell DM: Relationship between fibroblastic foci profusion and high  
430 resolution CT morphology in fibrotic lung disease. *BMC Med* 2015, 13:241.

431 [31] Piciucchi S, Tomassetti S, Ravaglia C, Gurioli C, Gurioli C, Dubini A, Carloni A, Chilosi  
432 M, Colby TV, Poletti V: From "traction bronchiectasis" to honeycombing in idiopathic  
433 pulmonary fibrosis: A spectrum of bronchiolar remodeling also in radiology? *BMC Pulm Med*  
434 2016, 16:87.

435 [32] Hunninghake GM, Hatabu H, Okajima Y, Gao W, Dupuis J, Latourelle JC, Nishino M,  
436 Araki T, Zazueta OE, Kurugol S, Ross JC, San Jose Estepar R, Murphy E, Steele MP, Loyd JE,  
437 Schwarz MI, Fingerlin TE, Rosas IO, Washko GR, O'Connor GT, Schwartz DA: MUC5B  
438 promoter polymorphism and interstitial lung abnormalities. *N Engl J Med* 2013, 368:2192-200.

439 [33] Seibold MA, Smith RW, Urbanek C, Groshong SD, Cosgrove GP, Brown KK, Schwarz  
440 MI, Schwartz DA, Reynolds SD: The idiopathic pulmonary fibrosis honeycomb cyst contains  
441 a mucociliary pseudostratified epithelium. *PLoS One* 2013, 8:e58658.

442 [34] Scotton CJ, Chambers RC: Molecular targets in pulmonary fibrosis: the myofibroblast in  
 443 focus. *Chest* 2007, 132:1311-21.

444 [35] Blackwell TS, Tager AM, Borok Z, Moore BB, Schwartz DA, Anstrom KJ, Bar-Joseph Z,  
 445 Bitterman P, Blackburn MR, Bradford W, Brown KK, Chapman HA, Collard HR, Cosgrove  
 446 GP, Deterding R, Doyle R, Flaherty KR, Garcia CK, Hagood JS, Henke CA, Herzog E,  
 447 Hogaboam CM, Horowitz JC, King TE, Jr., Loyd JE, Lawson WE, Marsh CB, Noble PW, Noth  
 448 I, Sheppard D, Olsson J, Ortiz LA, O'Riordan TG, Oury TD, Raghu G, Roman J, Sime PJ,  
 449 Sisson TH, Tschumperlin D, Violette SM, Weaver TE, Wells RG, White ES, Kaminski N,  
 450 Martinez FJ, Wynn TA, Thannickal VJ, Eu JP: Future directions in idiopathic pulmonary  
 451 fibrosis research. An NHLBI workshop report. *Am J Respir Crit Care Med* 2014, 189:214-22.

452 [36] Marchal-Somme J, Uzunhan Y, Marchand-Adam S, Valeyre D, Soumelis V, Crestani B,  
 453 Soler P: Cutting edge: nonproliferating mature immune cells form a novel type of organized  
 454 lymphoid structure in idiopathic pulmonary fibrosis. *J Immunol* 2006, 176:5735-9.

455 [37] Campbell DA, Poulter LW, Janossy G, du Bois RM: Immunohistological analysis of lung  
 456 tissue from patients with cryptogenic fibrosing alveolitis suggesting local expression of immune  
 457 hypersensitivity. *Thorax* 1985, 40:405-11.

458 [38] Idiopathic Pulmonary Fibrosis Clinical Research N, Raghu G, Anstrom KJ, King TE, Jr.,  
 459 Lasky JA, Martinez FJ: Prednisone, azathioprine, and N-acetylcysteine for pulmonary fibrosis.  
 460 *N Engl J Med* 2012, 366:1968-77.

461 [39] Zhang L, Wang Y, Wu G, Xiong W, Gu W, Wang CY: Macrophages: friend or foe in  
 462 idiopathic pulmonary fibrosis? *Respir Res* 2018, 19:170.

463 [40] Allden SJ, Ogger PP, Ghai P, McErlean P, Hewitt R, Toshner R, Walker SA, Saunders P,  
 464 Kingston S, Molyneaux PL, Maher TM, Lloyd CM, Byrne AJ: The Transferrin Receptor CD71  
 465 Delineates Functionally Distinct Airway Macrophage Subsets during Idiopathic Pulmonary  
 466 Fibrosis. *Am J Respir Crit Care Med* 2019, 200:209-19.

467 [41] Song E, Ouyang N, Horbelt M, Antus B, Wang M, Exton MS: Influence of alternatively  
468 and classically activated macrophages on fibrogenic activities of human fibroblasts. *Cell*  
469 *Immunol* 2000, 204:19-28.

470

471

## Figure legend

### Figure 1. Examples of pathological scores on IPF tissue section

H&E staining. (A) Mild patchy fibrosis (score=1) without honeycomb cysts formation (score=0) or emphysema (score=0). (B) Severe patchy fibrosis (score=3) without honeycomb cysts formation (score=0) or emphysema (score=0). (C) Mild patchy fibrosis (score=1) and emphysema (score=1) without honeycomb cysts formation (score=0). (D) Severe patchy fibrosis (score=3) and honeycomb (score=1) without emphysema (score=0). Scale bar indicates 2mm.

### Figure 2. Comparisons of microCT measures between regions with and without honeycomb cysts formation in IPF samples.

H&E staining. (A) Patchy fibrosis (score =2) without honeycomb cysts formation (score=0). (B) Patchy fibrosis (score =2) with honeycomb cysts formation (score = 1). Arrow indicates honeycomb region. The histological sections were matched with microCT images. (C and D) The alveolar surface density and number of terminal bronchioles per ml lung volume on microCT were decreased in honeycomb regions (n=12) compared to non-honeycomb regions (n=47). \* indicates  $p<0.05$ . (E) Three-dimensional rendering of the small airway tree (pink) overlaid onto microCT images from the same stack as used in panel B (see also online supplemental video 1). The small airway was connected with airspace in the honeycomb region (orange).

495

496 **Figure 3. Comparisons of alveolar surface density and number of terminal bronchioles**  
497 **between non-emphysematous regions with and without honeycomb cysts formation.**

498 (A) The alveolar surface density and (B) Number of terminal bronchioles were compared  
499 between control, non-emphysematous IPF samples with and without honeycomb regions (n=36,  
500 10, and 23). The absence of emphysema was determined based on the histological emphysema  
501 score of 0. \* indicates  $p<0.05$  compared to controls. † indicates  $p<0.05$  compared to non-  
502 emphysematous IPF samples without honeycomb regions.

503

## Tables

**Table1. Demographic data of subjects**

	Control (N=6)	IPF (N=10)
Age	58 ± 10	57 ± 5
Height (cm)	175 ± 6	173 ± 7
Weight (kg)	80 ± 15	73 ± 10
Sex	M : F = 6 : 0	M : F = 10 : 0
Smoking history	F : N = 2 : 4	F : N = 10 : 0
FEV <sub>1</sub> (% predicted)	NA	61 ± 15
FVC (% predicted)	NA	59 ± 20
D <sub>LCO</sub> (% predicted)	NA	28 ± 8

IPF = idiopathic pulmonary fibrosis. M : F = Male : Female. F : N = Former smoker : Never smoker. FEV<sub>1</sub> = forced expiratory volume in one second, FVC= Forced vital capacity, D<sub>LCO</sub>= diffusing capacity for carbon monoxide.



513 **Table2. Comparisons of microCT and histological findings between control and IPF**

	Control	IPF
No. tissue cores	36	60
MicroCT		
Alveolar surface density (/mm)	15.5 ± 2.0	8.9 ± 3.6**
Tissue% (%)	28.4 ± 3.7	50.5 ± 14.2**
Lm (um)	360 ± 53	529 ± 298**
No. terminal bronchioles/ml lung	4.1 ± 1.6	1.8 ± 1.3**
Histology scoring		
Patchy fibrosis	NA	1.3 ± 1.0
Fibroblastic Foci	NA	0.8 ± 0.8
Honeycomb	NA	0.2 ± 0.5
CD68	0.7 ± 0.5	1.6 ± 0.6**
CD4	0.4 ± 0.6	1.6 ± 0.7**
CD8	1.1 ± 0.4	1.6 ± 0.6**
CD79a	0.1 ± 0.3	1.2 ± 0.8**
Lymphoid follicle	0 ± 0	0.8 ± 0.8**

514 Tissue%=total lung volume taken up by tissue, Lm =the mean linear intercept. All scores range  
515 from 0 to 3. NA = not available. \*\*<p<0.005.

516

**Table 3. Spearman correlation coefficients between microCT indices and pathological scores in IPF samples**

	Alveolar surface density	Tissue%	Lm	No. terminal bronchioles
Major criteria for UIP				
Patchy fibrosis	-0.66**	0.69**	0.41**	-0.02
Fibroblastic foci	-0.52**	0.58**	0.39**	0.05
Honeycomb	-0.53**	0.38**	0.40**	-0.34**
Other scores				
Emphysema	0.01	-0.56**	0.19	-0.09
Inflammation	-0.25	0.31*	-0.03	0.09
Hyaline membrane	0.01	0.06	-0.13	0.00
Respiratory bronchiolitis	0.18	-0.17	-0.14	0.00

Tissue%=total lung volume taken up by tissue, Lm =the mean linear intercept.

\*p<0.05, \*\*<p<0.005.

523

524 **Table 4. Spearman correlation coefficients between microCT indices and scores of**  
 525 **infiltrated inflammatory immune cells in IPF samples**

	Alveolar surface density	Tissue%	Lm	No. terminal bronchioles
CD68	-0.20	0.49**	0.02	0.20
CD4	-0.11	0.30*	0.09	0.19
CD8	-0.17	0.41**	0.05	0.09
CD79a	-0.44**	0.53**	0.19	0.03
Lymphoid follicle	-0.41**	0.44**	0.14	-0.06

526 Tissue%=total lung volume taken up by tissue, Lm =the mean linear intercept.

527 \*p<0.05, \*\*<p<0.005.

528

Figure I

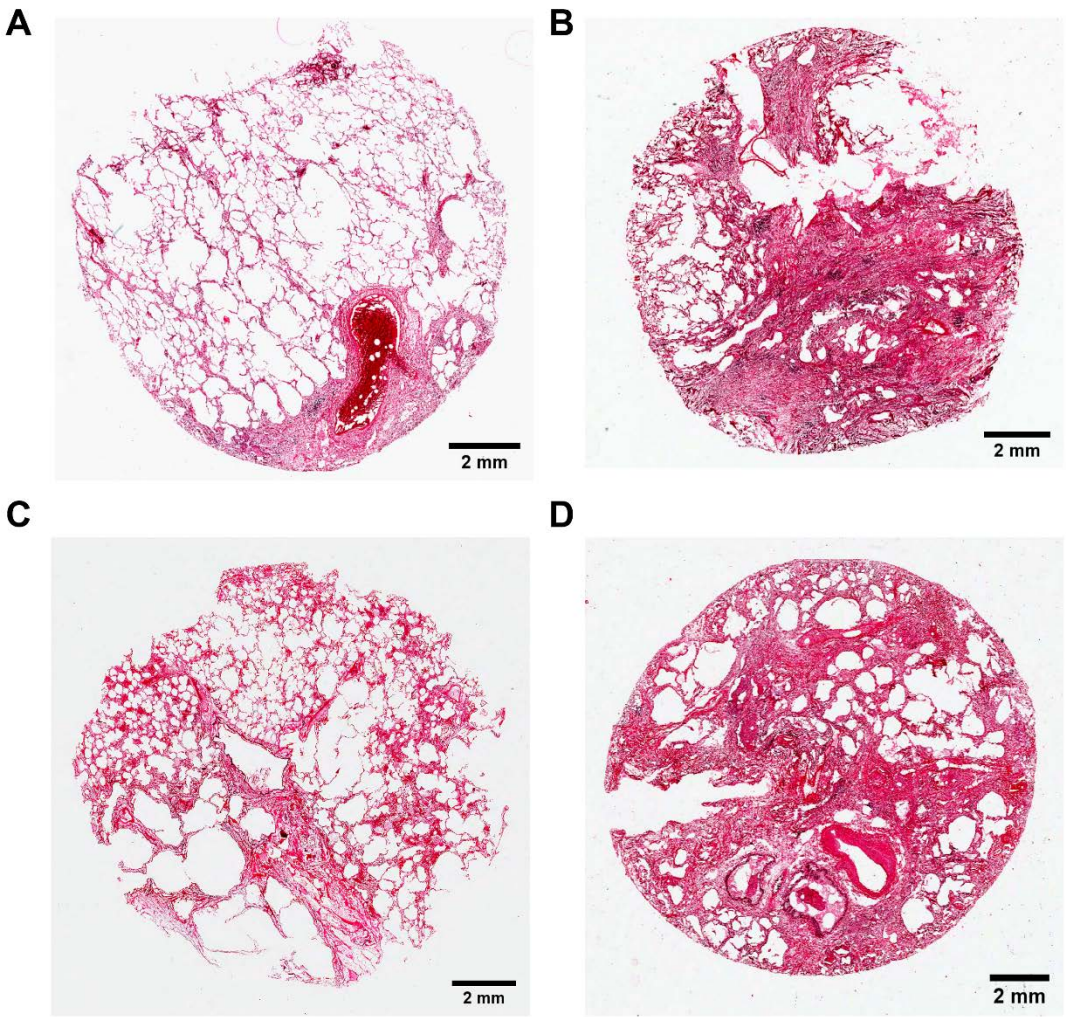


Figure 2

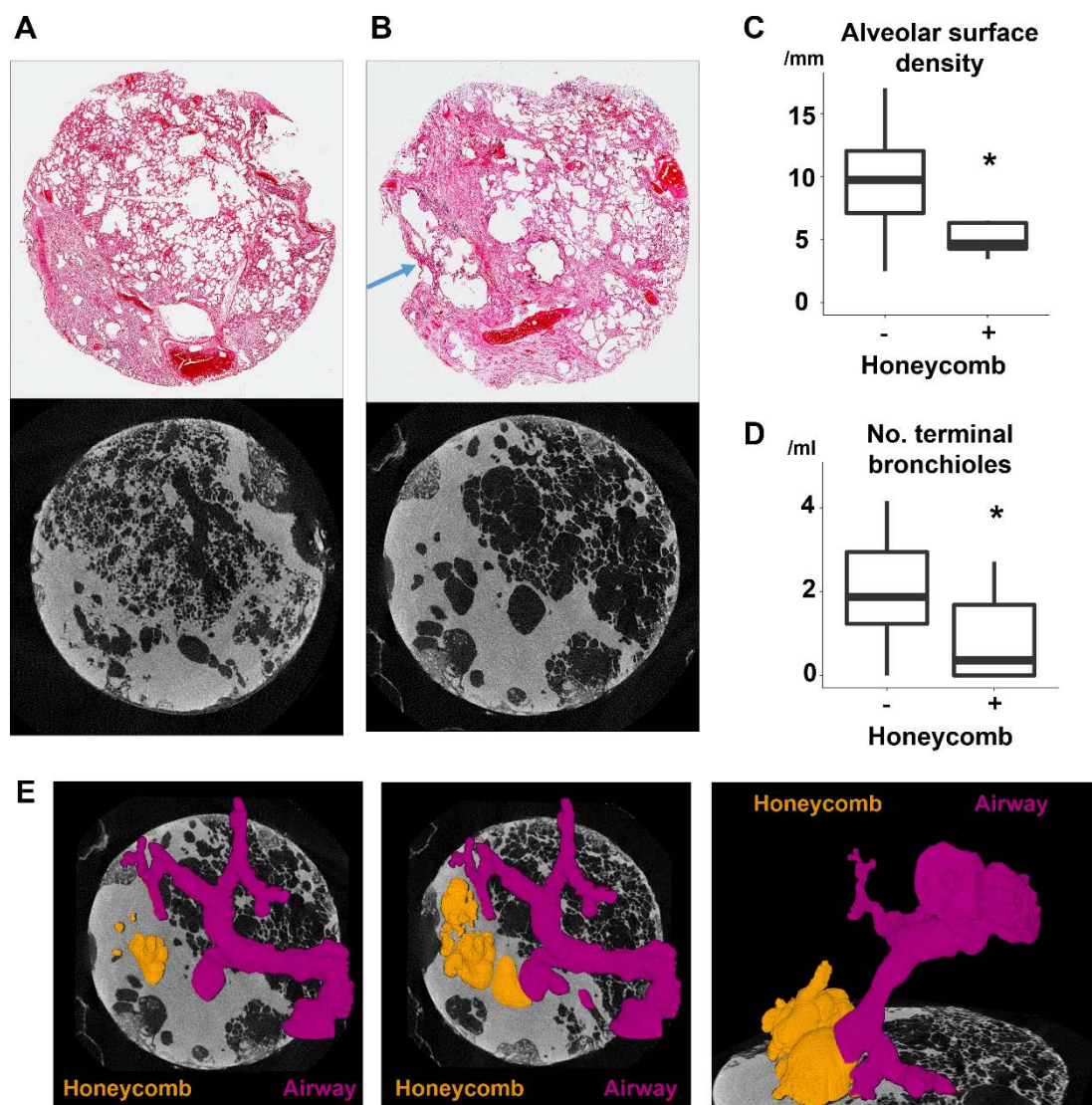


Figure 3

